JOURNAL OF GEOPHYSICAL RESEARCH, VOL. 105, NO. D3, PAGES 4077–4086, FEBRUARY 16, 2000

Parameterization of cold-season processes in the MAPS land-surface scheme

Tatiana G. Smirnova,[1] John M. Brown, Stanley G. Benjamin, and Dongsoo Kim[1]
NOAA Forecast Systems Laboratory, Boulder, Colorado

Abstract. A coupled atmospheric/land-surface model covering the conterminous United States with an associated 1-hour atmospheric data assimilation cycle, the Mesoscale Analysis and Prediction System (MAPS), has been improved to include a snow accumulation/melting scheme and also parameterization of processes in frozen soil. The new aspects of the land-surface model are described in this paper, along with detailed one-dimensional (1-D) tests using an 18-year observation data set from Valday, Russia. These tests show that the MAPS 1-D soil/vegetation/snow model is capable of providing accurate simulations over multiyear periods at locations with significant snow cover and frozen soil. A statistical analysis of the tests shows the expected improvement in snow depth, skin temperature, and especially in runoff from inclusion of these additional surface processes during the spring melting season. This performance in 1-D tests is a necessary prerequisite for robust long-term behavior of soil temperature and moisture fields and other components of the hydrological cycle in the 3-D MAPS coupled assimilation cycle.

1. Introduction

The development of improved capabilities for climate prediction and climate impact assessment requires a better understanding of the time and space variability of water and energy budgets over continental and subcontinental regions. To meet this goal, it is necessary to develop and validate high-resolution coupled atmospheric/land-surface models and also to develop methods for initializing them. The initialization consists of assimilation of diverse observations in the atmosphere and at the surface, consistent with the complex physical relationships in these systems. This issue was discussed in the scientific plan for the GEWEX (Global Energy and Water Cycle Experiment) Continental-Scale International Project (GCIP) [*World Meteorological Organization (WMO)*, 1992; *International GEWEX Project Office*, 1993].

The Mesoscale Analysis and Prediction System (MAPS) [*Benjamin et al.*, 1998, 1999] is a state-of-the-art coupled model and data assimilation system operating over the coterminous United States and producing grids for the GCIP. MAPS was developed at the NOAA Forecast Systems Laboratory (FSL) where it is run on a real-time continuous basis. It has also been implemented in a fully operational mode at the National Centers for Environmental Prediction (NCEP) as the Rapid Update Cycle or RUC. The 40-km, 40-level MAPS has been producing Model Output Reduced Data Set (MORDS) grids for GCIP since May 1996. MAPS is unique in that it provides these grids from an ongoing 1-hour assimilation cycle, including evolution of soil moisture and temperature. These observations used in MAPS include those from rawinsondes, surface atmospheric observation stations, commercial aircraft, wind profilers, and geostationary satellites. A summary of the characteristics of the 40-km MAPS is provided in more detail by *Benjamin et al.* [1998, 1999].

An initial five-level version of a land-surface soil/vegetation scheme [*Smirnova et al.*, 1997b] was incorporated into the ongoing MAPS assimilation cycle in early 1996 to improve its predictions of surface fluxes and atmospheric boundary layer properties by explicitly predicting soil moisture and temperature in a data assimilation cycle rather than depending on climatological soil moisture values, which can be seriously in error during and after dry or rainy periods. A newer six-level soil/vegetation/snow version, including processes in frozen soil, was tested in long-term integrations in a Project for the Intercomparison of Land-Surface Prediction Schemes (PILPS) [*Schlosser et al.*, 1999] mode using a 1-D configuration of MAPS/RUC.

The level of complexity of a land-surface process model to use within a coupled model such as MAPS is governed by the trade-off between computational efficiency and the best possible accuracy in describing physical processes. This same trade-off determines other central aspects of the MAPS configuration such as horizontal resolution and complexity of cloud and radiation physics. Thus the MAPS land-surface process model uses relatively simple treatment of frozen soil and snow physics. However, as we will show below, this treatment is able to produce relatively good results in controlled 1-D tests.

For GCIP a key question is the degree to which a coupled atmospheric/land-surface model, constrained by hourly assimilation of atmospheric observations to follow the evolution of the atmosphere accurately, can provide a realistic evolution of hydrological fields and time-varying soil fields that are not observed over large areas. A prerequisite for success is that the soil/vegetation/snow component of the coupled model, which is constrained only by atmospheric boundary conditions and definition of fields such as vegetation type and fraction and soil type, must be sufficiently robust to avoid drift over long periods of time. The land surface component of this model must also account for cold-season processes important in middle and

[1]Also at Cooperative Institute for Research in Environmental Sciences, Boulder, Colorado.

Paper number 1999JD901047.
0148-0227/00/1999JD901047$09.00

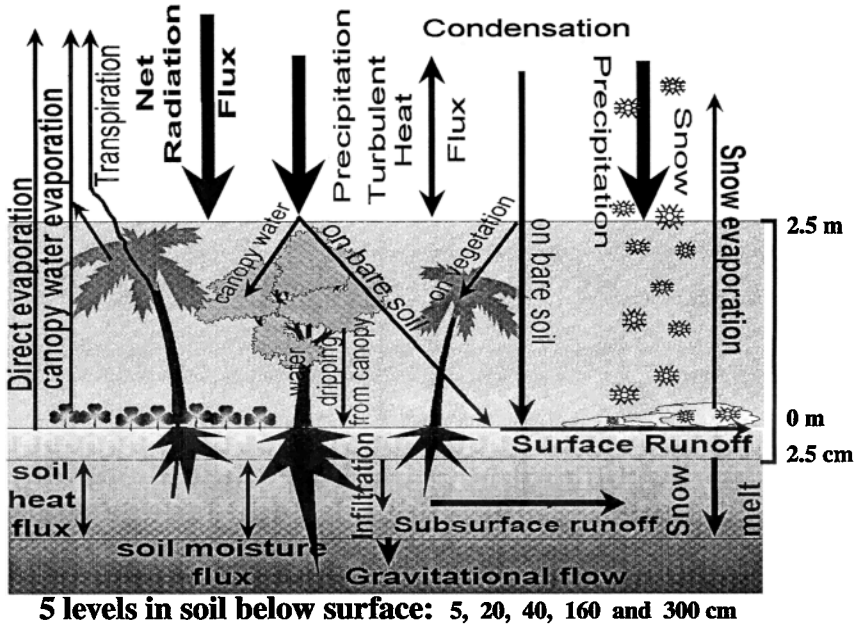

Figure 1. A summary of the processes in the Mesoscale Analysis and Prediction System/Rapid Update Cycle (MAPS/RUC) soil/snow/vegetation scheme.

high latitudes. One-dimensional tests of land-surface process models initialized with and verified against multiyear soil data sets with observed atmospheric forcing provide a controlled environment to examine model behavior. Therefore the focus of this paper is a complete description and validation of the 1-D land-surface process model with frozen soil and snow parameterizations used in the coupled MAPS assimilation/forecast system. In section 2 of this paper the most recent version of the soil/vegetation/snow model in MAPS is described. Detailed tests of this land-surface process model in a 1-D framework are presented in section 3. Concluding remarks are presented in section 4.

2. Soil/Vegetation/Snow Model Description

The MAPS/RUC soil model contains heat and moisture transfer equations together with the energy and moisture budget equations for the ground surface and uses an implicit scheme for the computation of the surface fluxes [*Smirnova et al.*, 1997a, b]. The heat and moisture budgets are applied to a thin layer spanning the ground surface and including both the soil and the atmosphere with corresponding heat capacities and densities (Figure 1). The version of this model tested in 1-D tests and running in the ongoing MAPS 3-D assimilation cycle has six levels, ranging from soil surface to 3 m in depth. A relatively simple concept for treating the evapotranspiration process [*Pan and Mahrt*, 1987], appropriate for use in an operational weather forecast model, is implemented in the MAPS/RUC soil/vegetation scheme. It partitions the total evaporation into three components: direct evaporation from the top layer of bare soil, evaporation of water directly from the vegetation canopy, and transpiration by plants involving water stored in the root zone of soil. Further enhancements of the MAPS/RUC soil/vegetation scheme are addressed below.

2.1. Parameterization of Snow Accumulation and Snow Melting

To improve MAPS/RUC prediction of skin temperature and surface air temperature in the cold season and to avoid significant errors that may result even at short timescales from inaccurate forecasts of snow cover, a scheme for computing snow accumulation on the ground surface and snow melting [*Smirnova et al.*, 1998] has been added to the soil/vegetation scheme initially described by *Smirnova et al.* [1997b].

When snow is present, snow is considered to be an additional one or two layers of soil depending on how deep it is. The snow depth is defined from the budget of water in solid form, assuming the constant value of snow density (set equal to 400 kg/m^3, typical value for old snow). The integrated form of this budget equation can be written as follows:

$$\rho_{sn}\frac{\partial h_{sn}}{\partial t} = (P_s - E)|_{\Delta z_a} - \rho_l M_t|_{sn-\mathrm{air}} - \rho_l M_b|_{sn-\mathrm{soil}}. \quad (1)$$

Here h_{sn} is snow depth, P_s is flux of liquid equivalent of solid precipitation, E is flux of water vapor sublimation/deposition from/onto the snow surface, M_t is a melting rate at snow-air interface, and M_b is a melting rate at snow-soil interface. A list of symbols is given in the Notation section.

Melting of snow cover from the top or bottom of snowpack is defined by solving energy budgets at the corresponding interface. First, an energy budget equation is solved for a thin layer spanning the top surface of the snowpack. This budget is applied to the half of the entire snow layer if snow depth computed from (1) is less than a threshold (currently set equal to 7.5 cm). For a more accurate solution of the energy budget through deeper snow, a snowpack thicker than 7.5 cm is split up into two layers, where the top layer is set to be 7.5 cm deep, and the energy budget is applied to the half of this top layer. This energy budget equation can be written as follows:

$$(\rho_a c_p \Delta z_a + \rho_{sn} c_{sn} \Delta z_{sn})\frac{\partial T_{sn}}{\partial t} = \{R_n + H_{\mathrm{rain}} - H - F - L_s \cdot [E_{\mathrm{dir}}(1-\sigma_f) + E_c\sigma_f] + L_v E_t \sigma_f\}|_{\Delta z_a} - G_{sn}|_{-\Delta z_{sn}}, \quad (2)$$

where T_{sn} is the mean temperature of a thin layer spanning the surface of the snow, R_n is net radiation flux into the layer, H_{rain}

is heat brought in to the ground surface by the liquid phase of precipitation, H is sensible heat flux to the atmosphere, F is latent heat required to melt snow, L_s is latent heat of sublimation, L_v is latent heat of evaporation, E_{dir} is sublimation/deposition flux from snow cover over bare soil, E_c is sublimation/deposition flux from snow on the canopy, E_t is transpiration flux, G_{sn} is heat flux into the snow, and σ_f is fraction of grid box covered by vegetation. (In the cold season σ_f can be very small or even zero. In the 3-D MAPS, σ_f is defined with the monthly satellite-based normalized differential vegetation index (NDVI) 0.14° data set of *Gutman and Ignatov* [1998]).

The heat flux into the snow in (2) is defined by

$$G_{sn} = \nu_{sn} \frac{T_{sn} - T_s}{h'_{sn}}, \tag{3}$$

where ν_{sn} is thermal conductivity of snow (set equal to a constant value of 0.35 W K^{-1} m^{-1}, which lies within the range of this variable for new and old snow [*Pielke*, 1984, Table 11-3]); T_s is the temperature at the soil-snow interface or, if the depth of snow is greater than threshold depth, snow temperature at the threshold depth; h'_{sn} is the depth of the top snow layer or the depth of the entire snowpack. An analogous equation is also used to define the heat flux through the lower snow layer, if present.

Direct sublimation from the snow surface and sublimation of snow from the canopy are more significant components in (2) than transpiration, because even if some leaves remain on trees and the vegetation fraction is nonzero, the transpiration is suppressed by the cold temperatures. Snow sublimates at a potential rate unless all of the snow layer would sublimate before the end of the time step. In this case the sublimation rate is reduced to that which would just sublimate all the existing snow during the current time step. Melting at the top of the snowpack occurs if the energy budget (2) produces T_{sn} higher than the freezing temperature (0°C). In this case, the snow temperature is set equal to the freezing point, and the residual from the energy budget is used to melt snow ($F > 0$ in (2)).

The heat transfer equation is solved within the full soil/snow column, including a one- or two-layer snowpack, as described by *Smirnova et al.* [1997b]. Melting at the bottom of the snowpack occurs if the temperature at the soil-snow interface would otherwise rise above freezing; the melt is just sufficient to maintain the temperature at (0°C). Similarly, at the top of snow cover, the snow temperature at this boundary is set equal to the freezing point, and the residual energy is used to melt snow. Water from melting snow infiltrates into the soil, and if the infiltration rate exceeds a maximum infiltration rate, then the excess water becomes surface runoff. The maximum infiltration rate used in MAPS is taken from the simple water balance model of *Schaake et al.* [1996], using their empirical formulation of probability distributions of sub-grid-scale processes. Refreezing of meltwater within the snow cover and the storage of liquid water in the snow are not considered in the current version of the snow model. The liquid water, as well as rain that falls on the snow, is currently assumed to percolate immediately down through the snowpack and is available for infiltration at the snow-soil interface. Ignoring these processes causes the snowpack to be melted too rapidly and runoff to be overestimated during melting periods, particularly spring.

In the full MAPS 3-D model, the accumulation of snow on the ground surface is provided by the microphysics algorithm of the MAPS/RUC forecast scheme [*Reisner et al.*, 1998; *Brown et al.*, 1998]. It predicts the total amount of precipitation and also the distribution of precipitation between solid and liquid phases. The sub-grid-scale ("convective") parameterization scheme also contributes to the liquid precipitation. With or without snow cover, the liquid phase is infiltrated into the soil at a rate not exceeding the maximum infiltration rate, as described by *Schaake et al.* [1996], and the excess goes into surface runoff. The solid phase in the form of snow or graupel is a source term in (1) and is unavailable for the soil until melting begins.

The integrated finite-difference form of the water budget at the interface between snow and soil is written as

$$\rho_l \Delta z_s \frac{\partial \eta_g}{\partial t} = -W_s|_{-\Delta z_s} + (I_m + \sigma_f D - E_t \sigma_f)\rho_{\Delta z_a}, \tag{4}$$

where η_g is the volumetric soil moisture content in the top half of the first soil layer, W_s is the soil moisture flux through the middle of the top soil layer, and I_m is the infiltration flux into soil originating from snowmelt and the liquid portion of total precipitation flux. D is the excess water dripping from the vegetation canopy onto the soil when the canopy is saturated, defined by

$$D = \begin{cases} P_l + M_t + M_b, & C^* \geq S' \\ 0, & C^* < S' \end{cases}. \tag{5}$$

Here P_l is the flux of liquid precipitation, S' is the saturation water content for a canopy surface, and C^* is the actual canopy water content.

2.2. Parameterization of Processes in Frozen Soil

Frozen soil plays a significant role in the hydrology of many regions, decreasing infiltration into the soil and causing large runoff rates from otherwise mild rainfall or snowmelt events. Significant runoff over saturated and unprotected soils may cause extreme erosion that may threaten agricultural productivity and construction projects. The need to control runoff and erosion and to determine sensitivity of these processes to soil properties and types of crops and vegetation covering the ground surface has generated much attention to adequately modeling of freezing and thawing processes among hydrologists and soil scientists. Many methods to predict the depth and permeability of frozen soil dependent on the interrelated processes of heat and moisture transfer within the soil have been developed [*Harlan*, 1973; *Fuchs et al.*, 1978; *Jame and Norum*, 1980; *Flerchinger and Saxton*, 1989]. Many of the models have a high degree of sophistication, but simultaneous heat and mass transport require an iterative procedure for numerical solution, making these models computationally expensive and not practical at the present time for coupling with atmospheric models used operationally for weather forecasting. For these coupled operational forecast models, a parameterization of processes in frozen soil needs to describe freezing and thawing processes in a simple way to be computationally efficient. In winter 1997–1998 such a parameterization of processes in frozen soil was incorporated into the MAPS coupled atmospheric/surface forecast model and assimilation cycle after extensive testing in a 1-D framework. The 1-D testing of the current MAPS land-surface model is described in section 3.

Lukianov and Golovko [1957] proposed two simplifying assumptions for description of processes in frozen soil: that the only significant phase change occurs between liquid water and ice and that there is no flow of ice. On the basis of this assumption, a 1-D heat balance equation for a soil layer in

which both latent and sensible heat are transported by conduction can be written as [*Harlan*, 1973]

$$C\frac{\partial T}{\partial t} - L_f S_{li} = \frac{\partial}{\partial z}\nu_f \frac{\partial T}{\partial z}, \tag{6}$$

where L_f is the heat of fusion, ν_f is the thermal conductivity of the potentially frozen soil, and S_{li} is the rate of liquid mass transformation into ice defined as

$$S_{li} = -\rho_l \frac{\partial \eta_l}{\partial t}, \tag{7}$$

where ρ_l is the density of water, and η_l is the volumetric content of liquid phase in soil. Applying the definition of liquid mass transformation rate to (6), the heat balance equation becomes

$$C_a\frac{\partial T}{\partial t} = \frac{\partial}{\partial z}\nu_f \frac{\partial T}{\partial z}, \tag{8}$$

where C_a is called the apparent heat capacity and is equal to

$$C_a = C + \rho_l L_f \frac{\partial \eta_l}{\partial T}. \tag{9}$$

The slope of the soil-freezing characteristic curve $\partial\eta_l/\partial T$ with zero solute concentration in the soil solution can be obtained from [*Cary and Mayland*, 1972; *Flerchinger and Saxton*, 1989]

$$\eta_l = \eta_s\left[\frac{L_f(T - 273.15)}{gT\Psi_s}\right]^{-1/b}, \tag{10}$$

where η_s is the volumetric moisture content at saturation, Ψ_s is the moisture potential for saturated soil.

The heat capacity of the soil is calculated according to the weighted contribution of the dry soil, liquid water, and ice:

$$C = (1 - \eta_s)C_s + \eta_l C_l + \eta_i C_i. \tag{11}$$

The thermal conductivity ν_f for soils with partially frozen water is defined from [*Pressman*, 1994]

$$\nu_f = \nu\left(1 + \frac{\rho_i}{\rho_l}\eta_i\right), \tag{12}$$

where thermal conductivity for unfrozen soils ν is calculated as described by *Smirnova et al.* [1997b].

The water balance of a soil layer at subfreezing temperatures can be written in terms of total water mass concentration as

$$\frac{\partial \Theta}{\partial t} = \rho_l\left(\frac{\partial}{\partial z}D_f\frac{\partial \eta_l}{\partial z} + \frac{\partial K_f}{\partial z}\right), \tag{13}$$

where

$$\Theta = \begin{cases} \rho_l\eta_l, & (\eta_i = 0) \\ \rho_l\eta_l + \rho_i\eta_i, & (\eta_i > 0) \end{cases} \tag{14}$$

is the density of total water mass content, D_f is diffusional conductivity in the frozen soil, and K_f is hydraulic conductivity in the frozen soil. According to experimental data [*Jame and Norum*, 1980] the presence of ice in soil disrupts the established flow paths and therefore reduces the water flow speed, and the impeding factor is assumed to be a function of total ice content. This experimental data showed that this factor may increase exponentially from 1 for ice-free conditions to 1000 when ice content is greater than 20%. Results from *Bloomsburg and Wang* [1969] showed that hydraulic conductivity is zero if $(\eta_s - \rho_i/\rho_l\eta_i) < 0.13$. For the top soil layer this means that the infiltration rate becomes zero, and all available liquid from snowmelt or precipitation creates surface runoff. The formulations of hydraulic and diffusional conductivity used in MAPS are written as follows [*Pressman*, 1994]:

$$K_f = K_s\left(\frac{\Theta - \rho_i\eta_i}{\Theta_s - \rho_i\eta_i}\right)^{2b+3}\left(1 - \frac{\rho_i\eta_i}{\Theta - \Theta_r}\right)^a, \tag{15}$$

$$D_f = K_f\frac{\partial \Psi_f}{\partial \eta}, \tag{16}$$

$$\Psi_f = \Psi_s\left(\frac{\Theta_s - \rho_i\eta_i}{\Theta - \rho_i\eta_i}\right)^b\left(\frac{\Theta_s}{\Theta_s - \rho_i\eta_i}\right)^c. \tag{17}$$

Here K_f and D_f are hydraulic and diffusional conductivities in the frozen soil, respectively, K_s is the hydraulic conductivity at saturation, Θ_s and Θ_r are densities of maximum possible and minimum values of soil moisture content, respectively, b is the exponent in the *Clapp and Hornberger* [1978] parameterization, and a and c are empirical parameters. The parameters K_s, Ψ_s, Θ_s, Θ_r, and b are functions of 11 USDA (U.S. Department of Agriculture) textural classes of soil plus peat, as presented by *Clapp and Hornberger* [1978]. The parameters a and c are set equal to 1 and 3, respectively, for all soil types. In case there is no frozen soil water, (15)–(17) transform into formulations used in MAPS previously and described by *Smirnova et al.* [1997b].

3. One-Dimensional Experiment for Valday, Russia

The MAPS soil/vegetation/snow model was tested off line in a one-dimensional (1-D) setting before incorporation into the MAPS/RUC three-dimensional (3-D) forecast model. Testing of its snow model and parameterization of processes in frozen soil, in particular, required data from a site with a significant winter season, including data about snow cover on the ground surface. To obtain such data, the MAPS/RUC land surface scheme became one of 21 models participating in Phase 2d of the Project for the Intercomparison of Land-Surface Parameterization Schemes (PILPS). PILPS Phase 2d was focused on the performances of land-surface schemes in the cold season, and it used the hydrological data set obtained from the Valday water-balance research station in Russia (57°58′N, 33°14′E), located in a boreal forest area. This area is within a climatic zone of Russia having significant seasonal variations with an annual temperature range of 35°C and an annual average precipitation of 730 mm with the maximum in the summer and autumn months. In winter, temperatures fall below −10°C, and persistent snow typically covers the ground surface from November until April (Figure 2). The PILPS Phase 2d experiment used the observed meteorological and hydrological data for the Usadievskiy grassland catchment at Valday (0.36 km^2 in areal extent) where long-term hydrological measurements were taken. The soil composition at Usadievskiy is 56% loam, 28% sandy loam, and 16% sand. The vegetation type is grassland meadow with a rooting depth of 1 m. Soil and vegetation parameters are described by *Schlosser et al.* [1999, Table 2]. The continuous 18 years (1966–1983) of atmospheric forcing and hydrologic data are described in detail by *Vinnikov et al.* [1996] and *Schlosser et al.* [1997, 1999].

In the Valday experiment the model simulates moisture and heat transfers inside the soil, and interaction processes between the ground/snow surface and the atmosphere, including surface fluxes, snow accumulation, and snow melting, as driven

by atmospheric forcing. The data sets have a 3-hour frequency and are interpolated to 30-min intervals (the model time step) as prescribed by PILPS. The first year of simulation was repeated until an equilibrium state was reached, i.e., until the simulation results were no longer dependent on the initial conditions. The simulated soil moisture, surface runoff, evapotranspiration, and snow water equivalent were verified against the observed data to evaluate the performance of the model.

Two basic experiments were run covering the 18-year period for this study, with and without parameterization of processes in the frozen soil. First, to evaluate the mean impact of the parameterization of processes in the frozen soil the annual cycles over the 18-year period are averaged for different variables in Figure 3. They demonstrate that the incorporation of frozen soil processes into MAPS model, on average, particularly improves performance during the spring snow melting season. The dates when snow melting starts and ends are better simulated by the MAPS version with parameterization of phase changes in the frozen soil (Figure 3a), although the average date when snow accumulation begins in the fall is reasonably good in both versions of MAPS. The climate of the hydrological cycle components of the Valday catchment during the cold season is also affected by consideration of processes in the frozen soil (Figures 3b, 3c). The total runoff, including both the surface runoff and the root zone drainage, is higher when the melting of snow occurs with parameterization of processes in the thawing soil and verifies better against observations (Figure 3b). The seasonal variation of soil water stored in the top meter of the soil (Figure 3c) is captured in both versions of MAPS fairly well, demonstrating moist conditions from October to April and drying out in summer. The differences between the two MAPS versions are not significant in the simulation of monthly accumulated total evaporation (Figure 3d), and both are closer to the lower end in the range of observed values.

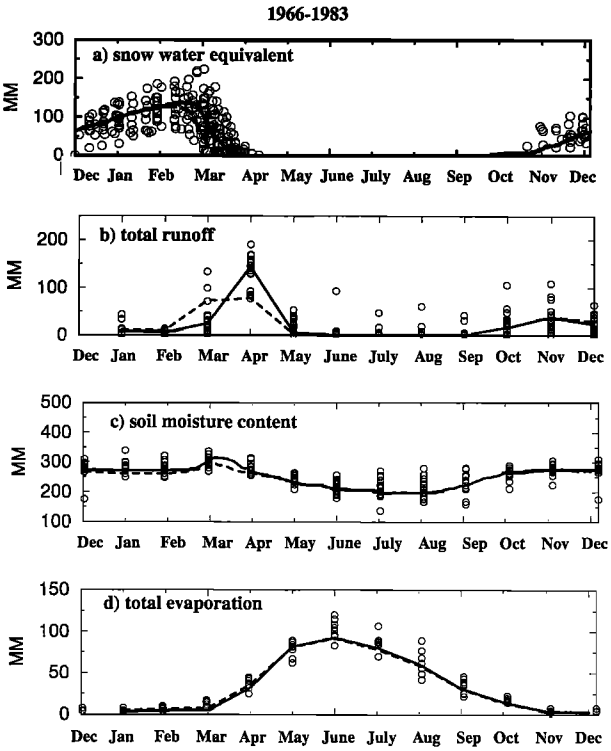

Figure 3. Annual variation of variables averaged in MAPS simulations with parameterization of processes in frozen soil (solid line) and without parameterization of processes in frozen soil (dashed line) over an 18-year period and observations (circles) for Valday, Russia. (a) Snow water equivalent, (b) total runoff from the root zone, (c) soil moisture content in the top 1-m layer, and (d) monthly accumulated total evaporation.

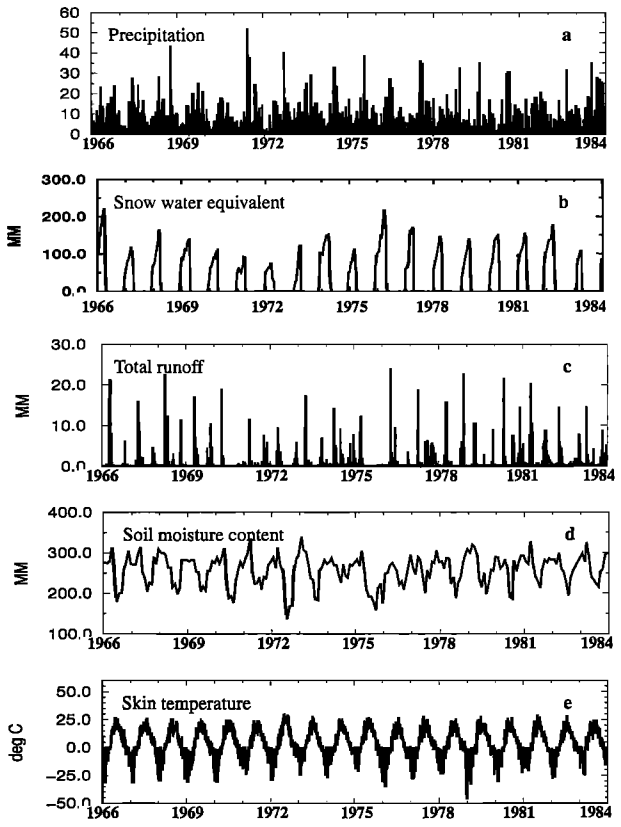

Figure 2. Observed annual variations for the years 1966–1983 of (a) daily precipitation (mm), (b) snow water equivalent, (c) total runoff from the root zone, (d) soil moisture content in the top 1-m layer, and (e) skin temperature for Valday, Russia.

Verification of model results for individual years of the 18-year period provides more details about the snow model performance under a variety of conditions ranging from dry winters with a maximum snow water equivalent of 74 mm to winters with snow water equivalent accumulation of more than 200 mm (Figure 4a). For most of the years, maximum snow accumulations for both versions of MAPS are close to the observed values, and the differences between the two are not significant. However, there are two winters with significant underestimation of snow accumulation: 20 mm in winter of 1967–1968 and 30 mm in winter of 1975–1976. There are also two winters when snow water equivalents at maximum snow accumulation are overestimated: 30 mm higher in winter of 1974–1975 and 40 mm higher in winter of 1980–1981. These large discrepancies between model simulations and observations may be connected to the interpretation of the atmospheric forcing, when precipitation is considered to be snow only at the below-freezing air temperatures at 2 m height. This assumption may be erroneous, especially in the late fall and early spring periods and may cause overestimation of snow

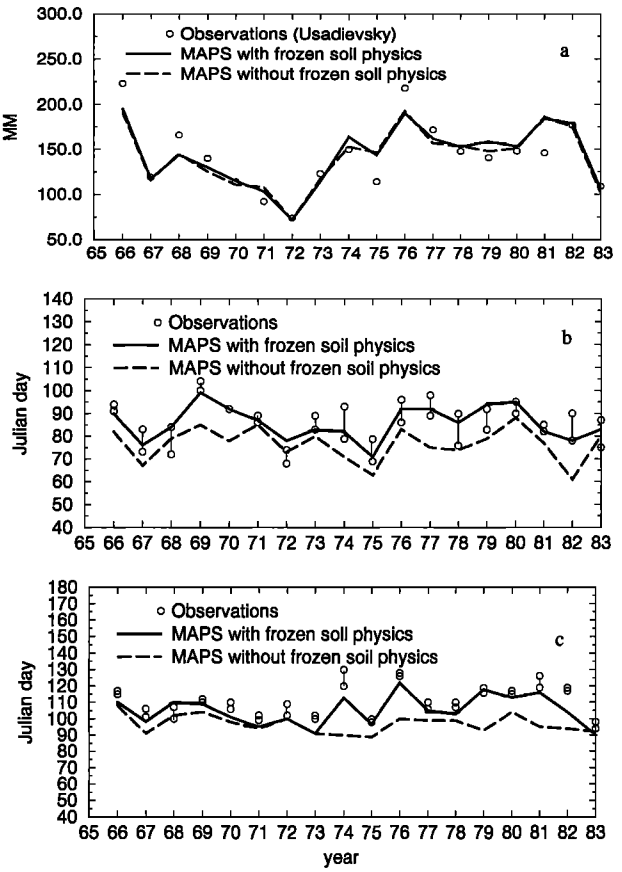

Figure 4. Interannual variability of variables observed (circles) and simulated in MAPS simulations with parameterization of processes in frozen soil (solid line) and without parameterization of processes in frozen soil (dashed line) for Valday, Russia. (a) Snow water equivalent, (b) dates when snow ablation starts, and (c) dates when snow pack is all melted.

accumulation as well as underestimation depending on the meteorological conditions.

The ability of the snow model to replicate the processes involved with the spring melting season can be verified by comparing the dates when the model ablation (spring melting) process starts and ends to the observed data (Figures 4b, 4c). Several days of separation (usually, up to 10 days, sometimes more) between observations of snow depth complicates defining the exact dates when the ablation process starts or all snow cover is melted at the Valday catchment. Therefore the observations on the plot are presented by the intervals defined from the available data. The frequency of snow observations also introduces some uncertainty in the definition of the date when the snowpack is all melted, especially for the years with late spring snow events. However, despite this uncertainty, Figure 4b and 4c demonstrate the positive impact of parameterizing processes in the frozen soil on the overall behavior of the land-surface scheme at this time of the year. With this parameterization the dates when the ablation of snowpack starts (Figure 4b) are delayed due to the colder temperatures of the underlying soil layers. The delays depend on the meteorological conditions and vary from 2 to 5 days in 1971, 1972, and 1973, the years with low snow accumulation and relatively early melting season, up to 10 days in 1969, 1977, and 1978, the years with high snow accumulation. The colder soil temperatures in this version of MAPS occur because soil with ice conducts heat from the deep soil layers forward to cold atmosphere faster due to a lower volumetric heat capacity compared to soil with water. Also, the parameterization of processes in the thawing soil spends energy from the surface energy budget on melting frozen water in the top soil layer, thereby reducing the residual energy that can be spent on snowmelt. Because of these factors the MAPS with this physics enhancement also improves the forecast dates when the snowpack is completely melted (Figure 4c). In the first half of the 18-year period these dates are only slightly more accurate with parameterization of processes in frozen soil, and even less accurate for 1968, when the end of the snow season is delayed too much. However, for the second half of the 18-year period the improvements are significant, but even with this improvement, the forecast snow season end date is earlier than observed for several years. This is attributable to simplified treatment of snow properties and to immediate infiltration of the melted water into the soil, which neglects the possibility of refreezing of melted water within the snowpack. It is also possible that spring snowfalls are mistakenly assigned to be rain in the atmospheric forcing based on above-freezing 2-m air temperatures, which may also contribute to the premature melting of the snowpack.

A statistical analysis comparing the two model simulations against independent observations during the spring seasons over all 18 years is performed for two variables: daily averaged skin temperature and daily accumulated total runoff from the top 1 m of soil (Table 1). The length of the melting period for each year over which statistics are calculated is shown in the first column of Table 1, and it varies from 12 days in 1969 and up to 50 days in 1974.

Analysis of statistics shows that the MAPS version with the parameterization of processes in the frozen soil produces more accurate skin temperatures for most of the years. For some

Table 1. Correlation Coefficients and Standard Deviations of Skin Temperature Differences Between Observations and Two MAPS Versions With ($Corr_f$, Std_f) and Without ($Corr_{nf}$, Std_{nf}) Parameterization of Processes in Frozen Soil, and Correlation Coefficients Between Observed and Simulated Total Runoff From the Top 1 m of Soil

	Length (Julian)	Skin Temperature				Runoff	
		$Corr_f$	$Corr_{nf}$	Std_f	Std_{nf}	$Corr_f$	$Corr_{nf}$
1966	91–117	0.954	0.828	1.271	2.019	0.485	−0.077
1967	73–103	0.921	0.915	1.389	1.423	0.498	−0.353
1968	74–106	0.935	0.883	1.714	1.904	−0.098	0.707
1969	100–112	0.965	0.939	1.968	1.609	0.546	−0.612
1970	92–110	0.870	0.684	1.693	1.780	0.699	0.025
1971	86–102	0.834	0.954	1.503	1.202	0.800	0.611
1972	75–108	0.961	0.960	1.735	1.668	0.553	0.305
1973	85–102	0.796	0.759	1.979	1.897	−0.126	−0.435
1974	80–130	0.946	0.811	1.618	2.929	0.549	−0.424
1975	58–100	0.930	0.936	1.712	1.666	0.617	−0.179
1976	99–127	0.872	0.374	2.065	4.166	0.906	−0.236
1977	91–110	0.847	0.656	1.813	2.640	0.745	−0.200
1978	77–110	0.946	0.904	1.787	2.163	0.587	0.172
1979	83–119	0.825	0.823	2.363	2.524	0.294	0.029
1980	91–116	0.942	0.834	1.475	2.296	0.556	−0.515
1981	92–126	0.925	0.719	1.436	2.597	0.857	−0.225
1982	79–119	0.902	0.821	1.744	2.246	0.728	−0.521
1983	64–98	0.944	0.949	2.583	2.491	0.588	0.234

Length is the spring melting period (Julian date) for which verification was performed.

years it produces close to the other version or slightly worse results. In 1971, 1972, and 1973, consistent with the small differences between the models in Figures 4b and 4c for these years, both versions of MAPS have close values of correlation coefficients for spring skin temperatures, the version without phase change in the thawing soil being slightly better in 1971. Standard deviations of skin temperature differences for these same three years are better in the simpler version of MAPS. These years are characterized by warm air temperatures, which causes (equations (7) and (10)) smaller amounts of soil water to be involved in the freezing-thawing processes. Therefore for these three snow melting seasons the importance of soil water phase changes is minimal. Similar results are also obtained for 1969 and 1975.

However, despite no improvement in skin temperature statistics for these years, parameterizing of processes in the frozen soil still produces improvement for simulation of total runoff, suggesting that the soil hydrology is captured better in this version of MAPS. The simulations of spring runoff events are significantly improved for 16 years, and there are only two years, 1968 and 1973, when this MAPS version fails to match the correct timing of spring runoff spike. One of these two years (1968) is the year when the other version of MAPS performs well and has a high value of the correlation coefficient between the spring runoff and the observations.

The internal consistency of hydrological cycle components in model simulations for some specific years helps to explain the statistics presented in Table 1. The winter season of 1971–1972

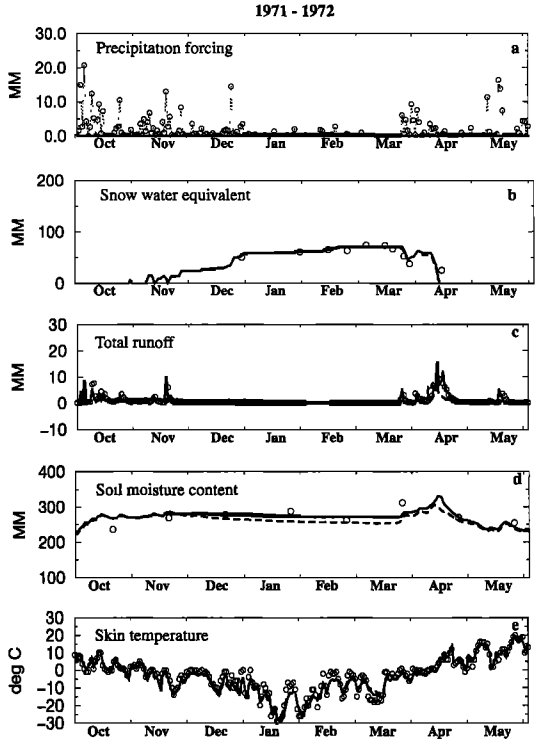

Figure 5. Variation of variables observed (circles) and simulated in MAPS simulations with parameterization of processes in frozen soil (solid line) and without parameterization of processes in frozen soil (dashed line) for Valday, Russia, winter 1971–1972. (a) Precipitation forcing from observations, (b) snow water equivalent, (c) total runoff from the top 1 m of soil, (d) soil moisture content in the top 1-m layer (root zone), and (e) skin temperature.

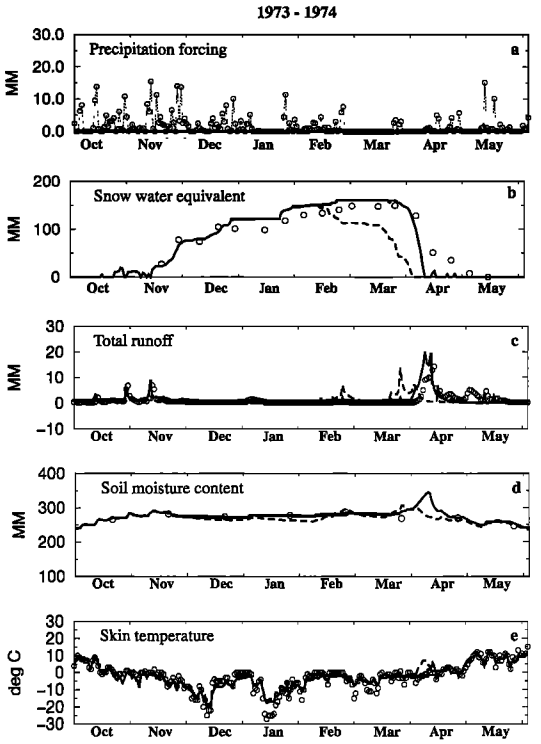

Figure 6. As in Figure 5 but for 1973–1974.

with the lowest observed snow depth during the 18-year simulation period (Figure 5b) exemplifies a dry winter. By the beginning of 1972, most of the snow had been already accumulated, and January and February were extremely dry months (Figure 5a). In March, melting of snow started, which was adequately reflected in the model behavior (Figure 5b), and in late March and early April, more fresh snow was accumulated on the ground. Incorporation of parameterization of processes in frozen soil into MAPS soil/snow model does not noticeably affect the accumulation and melting of snow for this year, and both versions of MAPS are able to simulate the snow depth consistent with observations. Major runoff events from the root zone of soil are also captured well in both versions of MAPS (Figure 5c) as reflected in high correlation coefficients (0.8 with and 0.611 without considering phase changes in frozen soil, Table 1). For the total amount of water in the top 1 m of soil the MAPS version with frozen soil physics is only slightly closer to the observed values (Figure 5d), and practically no discrepancies between the models can be noticed in the simulated daily averaged skin temperature (Figure 5e). All of these results are consistent with the relatively small importance of phase changes in soil for this year.

Larger differences between simulations from the two MAPS model versions occur for the 1973–1974 winter with average snow accumulation and long snow melting season (Figures 6a–6e). The model without parameterization of processes in frozen soil begins melting of snow too early compared to observations (Figure 6b). This is particularly reflected in the simulation of spring runoff, which peaks more than 2 weeks before observed. As a result, the amount of moisture stored in soil has an erroneous increase at the end of March (Figure 6d), and the skin temperature is overestimated at the beginning of April when all snow is melted in this version of MAPS (Figure 6e). Incorporation of frozen soil parameterization into the

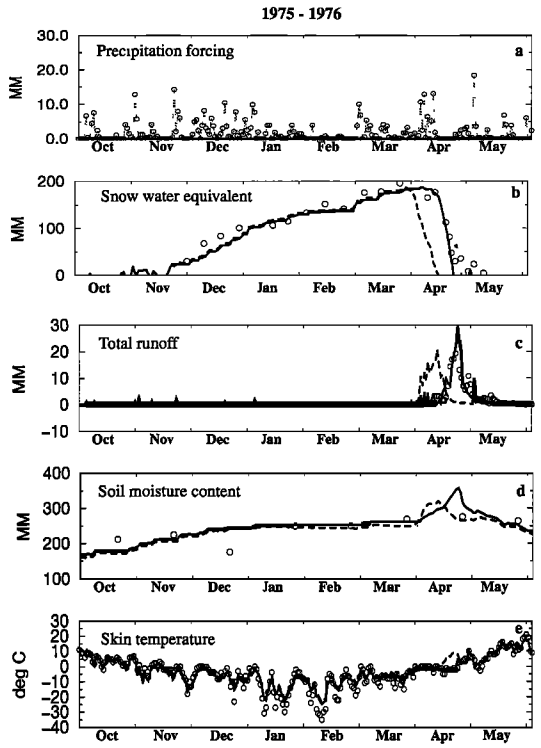

Figure 7. As in Figure 5 but for 1975–1976.

MAPS soil model has improved the model performance by delaying the beginning of the snow melting period (Figures 6b–6e and Figure 4b). Even in this version, the snowmelt is overestimated, so the snow season end date is too early (Figure 6b), and the spring runoff spike is too sharp and high (Figure 6c). However, the runoff spike is timed much more closely to the observed spike than in the other version of MAPS. The correlation coefficients between observed and simulated values of runoff are much higher for this melting season with the parameterization of processes in the frozen soil and are negative for the other model (Table 1). Relatively high values of snow depth in the observations for April 1974 suggest that April precipitation occurred in a form of snow, but the observed 2-m air temperatures show that most of it was interpreted as rain as prescribed in the experiment design. This contributes to reducing the length of the melting season as well as the simplified treatment of the snow properties and immediate infiltration of the melted water into the soil mentioned earlier.

Seasonal variations of these same variables in simulations for 1975–1976, a winter with higher than average snow cover, are depicted in Figure 7. Similar to 1973–1974 (Figures 6b, 6c), consideration of phase change in the soil has a positive impact on the simulation of spring snowmelt and spring runoff. The snow ablation with parameterization of processes in the frozen soil starts 10 days later than in the other version of MAPS (Figures 7b, 4b) considerably improving the model performance. The runoff is affected the most, and its spring spike matches the observations with a correlation coefficient 0.906, while for the other MAPS version, the correlation coefficient is negative (Table 1). Daily averaged skin temperatures in the two versions of MAPS noticeably differ only while the version of the model without frozen soil physics is simulating snow-free ground and the other still has snow cover (Figure 7e). In this situation, temperature differences become very large, and the skin temperature statistics for the version with the parameterization of the processes in the frozen soil are significantly improved (Table 1).

4. Concluding Remarks

The hydrological budget of land areas in middle and high latitudes is dominated much of the year by processes related to snow and subfreezing temperatures in the soil. To improve the handling of these processes in the MAPS coupled model producing gridded fields for GCIP, parameterizations for snow and frozen soil have been added. These parameterizations have been described in detail in this paper.

One-dimensional tests of this version of the MAPS land-surface model have been performed using observation data sets of 18 years from Valday, Russia, which is the focus of the PILPS 2-D test. Overall, the MAPS 1-D model gave good performance for this site, enhanced in several key aspects by the addition of a frozen soil parameterization. The main features in seasonal change of soil moisture, total runoff from the top 1 m of soil, and also snow accumulation and melting are affected positively by the addition of the parameterization of phase change in freezing and thawing soil. The most significant differences in the behavior of the models are observed during the snow melting season, which became the focus of a statistical analysis. This statistical analysis was limited by the availability of the observations and was performed for daily averaged skin temperature and the total runoff. The statistics for the skin temperature indicate that the importance of freezing/thawing processes varies with different types of winters. The skin temperature statistics are improved for the years with cold winter temperatures and high snow accumulation, which indicates that the addition of the frozen soil parameterization for such years provides improved contribution of the soil heat flux to the energy budget of the snowpack at the beginning of the snow ablation period. The years with warm winters and low snow accumulation have close values of correlation coefficients for both MAPS versions and slightly worse standard deviations of temperature differences in the model, which considers phase change in the frozen soil. The correlation coefficients between the simulated and observed total runoff show better results with the frozen soil parameterization for 16 years out of 18, and even for years when there are no improvements in the skin temperature simulations. This happens because the spring runoff spikes are more correlated with the dates when the snow ablation starts than with the thermal regime inside soil, and these dates are better captured in the version of MAPS considering phase changes of soil water. Further improvement in simulating the spring snow melting season may be achieved by more accurate treatment of snow properties and also by including storing and refreezing of melted water within the snowpack.

Some initial investigation has been performed to examine the variations of hydrological cycle components from the MAPS 3-D forecast/assimilation cycle. *Berbery et al.* [1999] report on comparisons of MAPS energy budget data with those from observations and other regional models, but the period studied is before the implementation of frozen soil physics in MAPS in March 1999. Future work will include use of new, higher-resolution soil and vegetation databases in the 3-D MAPS cycle, consideration of subgrid surface heterogeneity,

and a systematic evaluation of MAPS hydrological cycle data produced since the inclusion of frozen soil physics.

Notation

a, b, c empirical dimensionless factors dependent on soil type.
c_p specific heat capacity of air under constant pressure, J kg^{-1} K^{-1}.
c_{sn} specific heat capacity of snow, J kg^{-1} K^{-1}.
c_l specific heat capacity of water, J kg^{-1} K^{-1}.
C volumetric heat capacity of soil, J m^{-3} K^{-1}.
C_a apparent volumetric heat capacity of soil, J m^{-3} K^{-1}.
C_i volumetric heat capacity of ice, J m^{-3} K^{-1}.
C_l volumetric heat capacity of liquid water, J m^{-3} K^{-1}.
C_s volumetric heat capacity of dry soil, J m^{-3} K^{-1}.
C^* canopy water content, m.
D water drip flux from canopy to soil, kg m^{-2} s^{-1}.
D_f diffusional conductivity for frozen soil, m^2 s^{-1}.
E flux of water vapor sublimation/deposition, kg m^{-2} s^{-1}.
E_c flux of water vapor sublimation/deposition on the canopy snow, kg m^{-2} s^{-1}.
E_{dir} sublimation/deposition flux from snow cover over the bare soil, kg m^{-2} s^{-1}.
E_t transpiration flux, kg m^{-2} s^{-1}.
F heat of snow melting, W m^{-2}.
g acceleration of gravity, m s^{-2}.
G_{sn} heat flux into the snow, W m^{-2}.
H sensible heat flux from ground, W m^{-2}.
H_{rain} heat brought to the ground surface by liquid phase of precipitation, W m^{-2}.
$H_{\mathrm{rain}}=c_l P_l(T_{\mathrm{rain}} - T_{sn})$.
h_{sn} snow depth, m.
h'_{sn} depth of top snow layer or depth of entire snowpack, m.
I_m infiltration flux into soil, kg m^{-2} s^{-1}.
K_f hydraulic conductivity in frozen soil, m s^{-1}.
K_s saturated soil value of hydraulic conductivity, m s^{-1}.
L_f latent heat of fusion, J kg^{-1}.
L_s latent heat of sublimation, J kg^{-1}.
L_v latent heat of evaporation, J kg^{-1}.
M_b melting rate at the snow-soil interface, m s^{-1}.
M_t melting rate at the snow-air interface, m s^{-1}.
P_l flux of liquid precipitation, kg m^{-2} s^{-1}.
P_s flux of liquid equivalent of solid precipitation, kg m^{-2} s^{-1}.
R_n net radiation, W m^{-2}.
S_{li} rate of liquid mass transformation into ice, kg m^{-3} s^{-1}.
S' saturation water content for a canopy surface (= 0.005 m).
T temperature, K.
T_{rain} temperature of liquid precipitation set equal to temperature at the first atmospheric level.
T_{sn} temperature in a thin layer spanning the snow surface, K.
T_s temperature at the soil-snow interface or at the threshold depth within the snow, K.
Θ density of total soil moisture content, kg m^{-3}.
Θ_r density of minimum total soil moisture content, kg m^{-3}.
Θ_s density of maximum total soil moisture content, kg m^{-3}.
W_s moisture flux into the ground, kg m^{-2} s^{-1}.
z vertical coordinate, increasing upward, m.
Δz_a half of the lowest atmospheric model level height (5 m).
Δz_{sn} half of the snow depth, or half of the top snow layer, m.
Δz_s half of the top soil layer depth, m.
η volumetric water content of soil (dimensionless).
η_g volumetric water content of soil in the top half of first soil layer.
η_i volumetric content of ice in soil.
η_l volumetric content of liquid phase in soil.
η_s porosity of soil.
ν thermal conductivity of soil, W m^{-1} K^{-1}.
ν_f thermal conductivity of potentially frozen soil, W m^{-1} K^{-1}.
ν_{sn} thermal conductivity of snow, W m^{-1} K^{-1}.
Ψ_s moisture potential for saturated soil, m.
Ψ_f moisture potential for partially frozen soil, m.
ρ_a air density at the lowest model level, kg m^{-3}.
ρ_i density of ice (= 900), kg m^{-3}.
ρ_l density of liquid water (= 1000), kg m^{-3}.
ρ_{sn} snow density (= 400), kg m^{-3}.
σ_f nondimensional plant-shading factor.

Acknowledgments. The authors wish to thank Adam Schlosser and Alan Robock for their excellent assistance with use of the data sets for 1-D testing of the MAPS land-surface model. We also thank Barry Schwartz and Nita Fullerton for their excellent reviews of an earlier version of the manuscript. This work has been supported by grants from the NOAA Office of Global Programs and the NASA Mission to Planet Earth.

References

Benjamin, S. G., J. M. Brown, K. J. Brundage, B. E. Schwartz, T. G. Smirnova, and T. L. Smith, The operational RUC-2, in *16th Conference on Weather Analysis and Forecasting*, pp. 249–252, Am. Meteorol. Soc., Boston, Mass., 1998.

Benjamin, S. G., J. M. Brown, K. J. Brundage, D. Kim, B. E. Schwartz, T. G. Smirnova, and T. L. Smith, Aviation forecasts from the RUC-2, in *8th Conference on Aviation, Range, and Aerospace Meteorology*, pp. 486–490, Am. Meteorol. Soc., 1999.

Berbery, E. H., K. Mitchell, S. Benjamin, T. Smirnova, H. Ritchie, R. Hogue, and E. Radeva, Assessment of land-surface energy budgets from regional and global models, *J. Geophys. Res.*, *104*, 19,329–19,348, 1999.

Bloomsburg, G. L., and S. J. Wang, Effect of moisture content on permeability of frozen soils, in *Sixteenth Annual Meeting of Pacific Northwest Region*, AGU, Washington, D. C., 1969.

Brown, J. M., T. G. Smirnova, and S. G. Benjamin, Introduction of MM5 level 4 microphysics into the RUC-2, in *Twelfth Conference on Numerical Weather Prediction*, pp. 113–115, Am. Meteorol. Soc., Boston, Mass., 1998.

Cary, J. W., and H. F. Mayland, Salt and water movement in unsaturated frozen soil, *Soil Sci. Soc. Am. Proc.*, *36*, 549–555, 1972.

Clapp, R., and G. Hornberger, Empirical equations for some soil hydraulic properties, *Water Resour. Res.*, *14*, 601–604, 1978.

Flerchinger, G. N., and K. E. Saxton, Simultaneous heat and water model of a freezing snow-residue-soil system, I, Theory and development, *Trans. Am. Soc Agric. Eng.*, *32*(2), 565–571, 1989.

Fuchs, M., G. S. Campbell, and R. I. Papendick, An analysis of sensible and latent heat flow in a partially frozen unsaturated soil, *Soil Sci. Soc Am. J.*, *42*(3), 379–385, 1978.

Gutman, G., and A. Ignatov, The derivation of green vegetation fraction from NOAA/AVHRR for use in numerical weather prediction model, *Int. J. Remote Sens.*, *19*, 1533–1543, 1998.

Harlan, R. L., Analysis of coupled heat-fluid transport in partially frozen soil, *Water Resour. Res.*, *9*(5), 1314–1323, 1973.

International GEWEX Project Office, *Implementation Plan for the GEWEX Continental-Scale International Project (GCIP), Data Collection and Operational Model Upgrade*, vol. I, compiled and edited by J. A. Leese, 83 pp., Washington, D. C., 1993.

Jame, Y.-W., and D. I. Norum, Heat and mass transfer in a freezing unsaturated porous medium, *Water Resour. Res.*, *16*(4), 811–819, 1980.

Lukianov, V. S., and M. D. Golovko, Calculation of the depth of freeze in soils (in Russian), *Bull. 23*, Union of Transp. Constr., Moscow, 1957. (English transl., Natl. Tech. Inf. Serv., Springfield, Va.)

Pan, H.-L., and L. Mahrt, Interaction between soil hydrology and boundary-layer development, *Boundary Layer Meteorol.*, *38*, 185–202, 1987.

Pielke, R. A., *Mesoscale Meteorological Modeling*, 612 pp., Academic, San Diego, Calif., 1984.

Pressman, D. Y., Chislennaya model' gidrotermicheskikh protsessov v pochve kak chast' skhemi mesomasshtabnogo prognoza (Numerical model of hydrothermal processes in soil as a part of the scheme of mesoscale forecasting), *Meteorol. Gidrol.*, *11*, 62–75, 1994.

Reisner, J., R. M. Rasmussen, and R. T. Bruintjes, Explicit forecasting of supercooled liquid water in winter storms using the MM5 mesoscale model, *Q. J. R. Meteorol. Soc.*, *142*, 1071–1107, 1998.

Schaake, J. C., V. I. Koren, Q.-Y. Duan, K. Mitchell, and F. Chen, Simple water balance model for estimating runoff at different spatial and temporal scales, *J. Geophys. Res.*, *101*, 7461–7475, 1996.

Schlosser, C. A., A. Robock, K. Y. Vinnikov, N. A. Speranskaya, and Y. Xue, 18-year land surface hydrology model simulations for a midlatitude grassland catchment in Valdai, Russia, *Mon. Weather Rev.*, *125*, 3279–3296, 1997.

Schlosser, C. A., et al., Simulations of a boreal grassland hydrology at Valdai, Russia: PILPS Phase 2(d), *Mon. Weather Rev.*, in press, 1999.

Smirnova, T. G., J. M. Brown, and S. G. Benjamin, Evolution of soil moisture and temperature in the MAPS/RUC assimilation cycle, in *13th Conference on Hydrology*, pp. 172–175, Am. Meteorol. Soc., Boston, Mass., 1997a.

Smirnova, T. G., J. M. Brown, and S. G. Benjamin, Performance of different soil model configurations in simulating ground surface temperature and surface fluxes, *Mon. Weather Rev.*, *125*, 1870–1884, 1997b.

Smirnova, T. G., J. M. Brown, and S. G. Benjamin, Impact of a snow physics parameterization on short-range forecasts of skin temperature in MAPS/RUC, *Twelfth Conference on Numerical Weather Prediction*, pp. 161–164, Am. Meteorol. Soc., Boston, Mass., 1998.

Vinnikov, K. Y., A. Robock, N. A. Speranskaya, and C. A. Schlosser, Scales of temporal and spatial variability of midlatitude soil moisture, *J. Geophys. Res.*, *101*, 7163–7174, 1996.

World Meteorological Organization (WMO), Scientific Plan for the GEWEX Continental-Scale International Project (GCIP), *WCRP-67,WMO/TD-61*, 65 pp., Geneva, 1992.

S. G. Benjamin, J. M. Brown, D. Kim, and T. G. Smirnova, NOAA/ERL/FSL, R/E/FS1, 325 Broadway, Boulder, CO 80303. (smirnova@fsl.noaa.gov)

(Received March 29, 1999; revised September 21, 1999; accepted September 28, 1999.)